

Numerical simulation of possible laboratory measurements of water vapor continuum absorption in the near IR region

I.V. Ptashnik

*Institute of Atmospheric Optics,
Siberian Branch of the Russian Academy of Sciences, Tomsk*

Received October 11, 2005

Water vapor continuum absorption is an important component of molecular absorption of radiation in the atmosphere. However, the uncertainty in the value of continuum absorption in different spectral regions can achieve 100%, leading to errors in the flux calculation up to 3–5 W/m² (global mean). Based on line-by-line calculations, this paper presents optimal spectral intervals for laboratory verification of air-broadened water vapor continuum absorption in the near-infrared spectral region, in which the continuum absorption is studied most poorly today. Possible sources of systematic and random errors, taken into account in the simulation, include the spectrometer sensitivity and uncertainties in spectral line parameters in the HITRAN-2004 database.

Introduction

The so-called water vapor continuum absorption (or, simply, water vapor continuum), only slightly depending on the frequency, is a significant component of molecular absorption in the atmosphere and can contribute up to 10 W/m² or 5–6% to the total atmospheric absorption of the solar radiation.*

The CKD (Clough, Kneizys, and Davies) semi-empirical model of the continuum,¹ used now in the most radiative codes, defines the continuum absorption coefficient as follows

$$k_c(\bar{\nu}) = R(\bar{\nu}, T) \times \sum_i \{ S_i(T) [f_c(\bar{\nu} - \bar{\nu}_i) \chi(\bar{\nu} - \bar{\nu}_i) + f_c(\bar{\nu} + \bar{\nu}_i) \chi(\bar{\nu} + \bar{\nu}_i)] \};$$

$$f_c(\bar{\nu} \pm \bar{\nu}_i) = \begin{cases} \frac{1}{\pi} \frac{\gamma_i}{\Delta \bar{\nu}_{\text{cutoff}}^2 + \gamma_i^2}, & |\bar{\nu} \pm \bar{\nu}_i| \leq \Delta \bar{\nu}_{\text{cutoff}}, \\ \frac{1}{\pi} \frac{\gamma_i}{(\bar{\nu} \pm \bar{\nu}_i)^2 + \gamma_i^2}, & |\bar{\nu} \pm \bar{\nu}_i| > \Delta \bar{\nu}_{\text{cutoff}}, \end{cases} \quad (1)$$

where $\bar{\nu}$ is the wave number, in cm⁻¹; $R(\bar{\nu}, T)$ is the radiative term accounting for the induced radiation; $S_i(T)$ is the intensity of the i th transition; γ_i is the Lorentz half-width of a spectral line; $f_c(\bar{\nu} \pm \bar{\nu}_i)$ is the continual part of the line profile; $\Delta \bar{\nu}_{\text{cutoff}}$ is the distance from the line center, up to which the selective contribution of every line to absorption is taken into account (Fig. 1). In the CKD model, $\Delta \bar{\nu}_{\text{cutoff}} = 25 \text{ cm}^{-1}$. Parameters of the function $\chi(\bar{\nu} \pm \bar{\nu}_i)$ are determined by fitting the calculated spectrum to the experimental one and, according to the model,¹ give a correction to the impact theory due to the finite duration of molecular collisions.

* Hereinafter, the calculated results are presented for the mid-latitudinal summer conditions and the solar zenith angle of 30°.

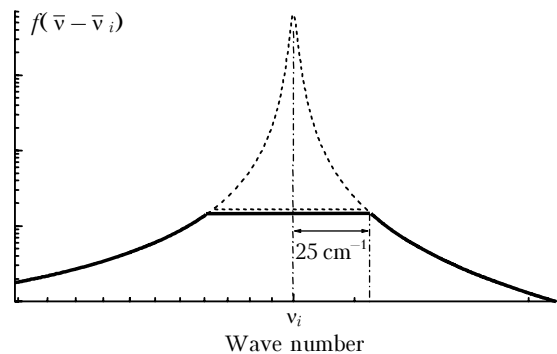


Fig. 1. Continual $f_c(\bar{\nu} - \bar{\nu}_i)$ (solid line) and selective (dashed line) parts of the absorption line profile in the CKD model.

In the two latest versions of the CKD model of continuum: CKD-2.4 [Ref. 2] and MT_CKD [Ref. 3] (http://rtweb.aer.com/continuum_frame.html), Mlawer with co-workers uses a somewhat different physical interpretation and parameterization of the function $k_c(\nu)$. In addition to the contribution of far wings of lines, corresponding to allowed transitions, determined by Eq. (1), the term describing transitions induced by collisions is included. Nevertheless, the absorption line profile used in the new CKD models of continuum is still described by the Voigt profile (calculated up to 25 cm⁻¹ from the line center) minus a constant background of continual absorption (see Fig. 1).

A good parameterization used in the CKD model of continuum has caused its wide usage in various atmospheric applications. Using the same type of the profile for all lines and several fitted parameters, the model provides for a more or less satisfactory agreement with the experiment in a wide spectral region.

Some investigators, however, have shown that the CKD model of continuum includes a significant degree of uncertainty, which manifests itself in comparing different versions of this model. This uncertainty may achieve 100% in some spectral ranges and causes the difference in the calculated integral absorbed solar radiation up to 2.5 to 3 W/m² [Refs. 4–7]. The

difference between the model continuum and the real absorption by far wings of spectral lines can be even larger. This is especially true in the near IR and visible regions, because until so far the parameters of the CKD model have been determined by fitting to the experiment only in the middle and far IR regions, that is, $> 4 \mu\text{m}$ ($0\text{--}2500 \text{ cm}^{-1}$) [Ref. 8–11], and have not undergone a somewhat reliable verification in the shortwave spectral region. Quite accurate measurements of the water vapor continuum absorption in the near IR region could also make clear the issue, which is still debated, of the physical nature of the continuum, in particular, as to the possible contribution of water dimers, which was discussed recently in Refs. 12 to 14.

Thus, the experimental verification of the CKD model of the continuum in the near IR and visible regions is still very urgent. Until recently, this has been connected with significant experimental difficulties, caused by very low continuum absorption in this spectral region. It can be seen from Fig. 2 that the water vapor continuum decreases quickly with the increasing wave number, not exceeding $10^{-6}\text{--}10^{-8} \text{ cm}^{-1}$ in line wings in the near IR region.

Five papers devoted to measurements of the water vapor continuum absorption in the visible and near IR regions are presently available. (Field measurements^{15,16} are not considered, because, as was shown in Ref. 17, the fine (soot) aerosol was likely the major contributor to nonselective absorption in that case.) Laboratory measurements of the water vapor continuum absorption in the transmission microwindows in the $3000\text{--}4200 \text{ cm}^{-1}$ band have been described in Ref. 18. Later these data were used to construct the first CKD model of continuum.¹

In Refs. 19 and 20, the nonresonant absorption of laser radiation by water vapor was measured at fixed wavelengths: 0.6943 and $1.056 \mu\text{m}$ (14399 and 9466 cm^{-1} , respectively). However, the influence of measurement errors and uncertainties in spectral line parameters from the HITRAN-96 database used in

the calculations was too large. Therefore, these measurements failed to refine considerably the value of continuum absorption in the spectral ranges studied.

Finally, quite recently the measurements of the water vapor continuum absorption along slant paths in the absorption bands at 0.72 and $0.94 \mu\text{m}$ (13900 and 10600 cm^{-1}) have been reported,²¹ as well as the laboratory measurements in the $1.89 \mu\text{m}$ (5300 cm^{-1}) absorption band.²²

These measurement results confirm the above thesis about the large uncertainty of the CKD model of continuum in the shortwave spectral range. Thus, for the $0.94 \mu\text{m}$ band the continuum absorption recorded in Ref. 21 proved to be 2 and 1.5 times lower than, respectively, in the CKD-2.4 and MT_CKD models. In the $0.72 \mu\text{m}$ band, the measured continuum appeared to be in a good agreement with the CKD-2.4 model, but 1.6 times higher than in the new MT_CKD model. About 1.5-fold excess over the CKD-2.4 model for the measured self-broadening continuum (in pure water vapor) was found in Ref. 22.

Significant progress achieved for the last 10 to 15 years in the high-resolution experimental laser spectroscopy, makes it possible, however, to extend considerably the spectral region of verification of the continuum absorption in the near IR spectral region. The methods of photoacoustic and cavity ring-down spectroscopy allow one to achieve the absorption sensitivity up to $10^{-9}\text{--}10^{-10} \text{ cm}^{-1}$.

Based on numerical simulation, this paper analyzes spectral ranges, optimal for the laboratory verification of the water vapor continuum absorption in the near IR region. The emphasis is put on the laboratory measurements, since the water continuum measured under field conditions often cannot be reconstructed with high accuracy because it is difficult to determine accurately the water vapor content on slant paths and to take into account the contribution coming to absorption from fine aerosol.

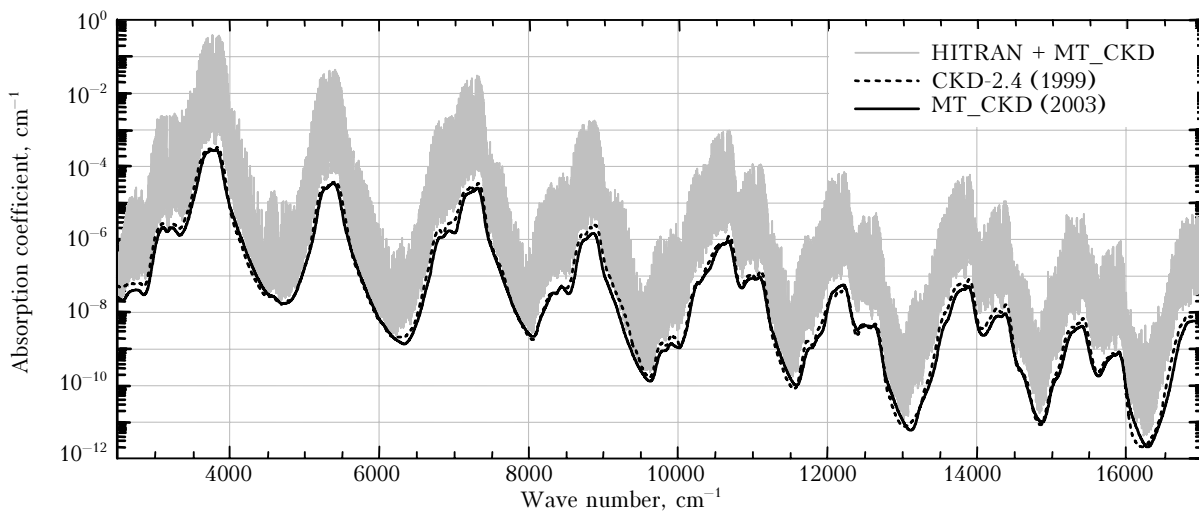


Fig. 2. CKD-2.4 [Ref. 2] and MT_CKD [Ref. 3] models of continuum for atmospheric conditions (H_2O pressure of 20 mbar, air pressure of 1013 mbar, 296 K) along with the water vapor absorption spectrum calculated with the use of the HITRAN-2004 database and MT_CKD continuum model.

Results obtained by simulation

To find spectral ranges, optimal for laboratory measurements of the continuum absorption, the calculations have been performed for a mixture of water vapor with air in the spectral region from 2500 to 15000 cm^{-1} (0.67–4 μm). For this purpose, the line-by-line code, developed at the Institute of Atmospheric Optics,²² was used. The results obtained by simulation are shown in Figs. 3–7. The calculations were performed for a mixture of 20 mbar of water vapor and 993 mbar of artificial air (80% N_2 and 20% O_2) in order to exclude the contributions from such gases as CO_2 , O_3 , and CH_4 . The simulation was carried out for the temperature of 296 K.

The top panels in Figs. 3–7 depict the spectra of absorption by water vapor spectral lines with and without the regard for the MT_CKD model of continuum (respectively, $K_{\text{Lines+MT_CKD}}$ and K_{Lines}). The latter version of calculation assumes the cut-off of a line profile within 25 cm^{-1} from the line center. The absorption according to the CKD-2.4 and MT_CKD models of continuum ($K_{\text{CKD-2.4}}$ and $K_{\text{MT_CKD}}$) is shown separately. The absorption by water vapor lines (K_{Lines}) is calculated using Schwenke–Partridge base of lines²³ with the parameters of the strongest lines taken from the HITRAN-2004 database.²⁴ This approach has allowed us to keep higher accuracy of the HITRAN-2004 parameters for strong spectral lines, as compared to the Schwenke–Partridge parameters, and to take into account large number of weak lines, absent now in the HITRAN database (for more details of this approach, see Refs. 5 and 7).

The bottom parts of Figs. 3–7 depict the spectra of the ratio of continuum absorption (according to

the MT_CKD model) to the absorption by water vapor spectral lines with continuum neglected (that is, $K_{\text{MT_CKD}}/K_{\text{Lines}}$), as well as the ratio $K_{\text{MT_CKD}}/\Delta K$, where ΔK is the estimated total error (experimental and calculated) of reconstruction of the continuum absorption. This error includes: a) possible systematic measurement error δ_{sys} (assumed equal to 0.03); b) random measurement error due to noise k_{noise} (assumed equal to $2 \cdot 10^{-9} \text{ cm}^{-1}$); c) error of consideration of the selective absorption by water vapor spectral lines due to inaccurate values of spectral line parameters in HITRAN-2004. In estimating the last error, the error codes, presented in the HITRAN database for line positions, intensities, air broadening and self-broadening coefficients, and temperature dependence, were taken into account. Thus, the error $\Delta K(\bar{\nu})$ was estimated as follows:

$$\Delta K(\bar{\nu}) = \left[\sum_{i=1}^4 \Delta k_i(\bar{\nu})^2 + k_{\text{noise}}^2 \right]^{1/2} + \delta_{\text{sys}} K_{\text{Lines+MT_CKD}}, \quad (2)$$

where Δk_i is the deviation of the calculated absorption coefficient from its initial value ($K_{\text{Lines+MT_CKD}}$) caused by the change of one of four line parameters (line position and pressure-induced shift coefficient, intensity, air broadening coefficient, and temperature dependence) on the uncertainty of this parameter according to the HITRAN-2004 error code (error codes in columns 128–133).

For weak Schwenke–Partridge lines,¹⁹ for which there is no accurate information about errors, the errors in the intensity, broadening coefficient, and temperature dependence were assumed equal to 30%, while the uncertainty in the line position was taken to be 0.2 cm^{-1} .

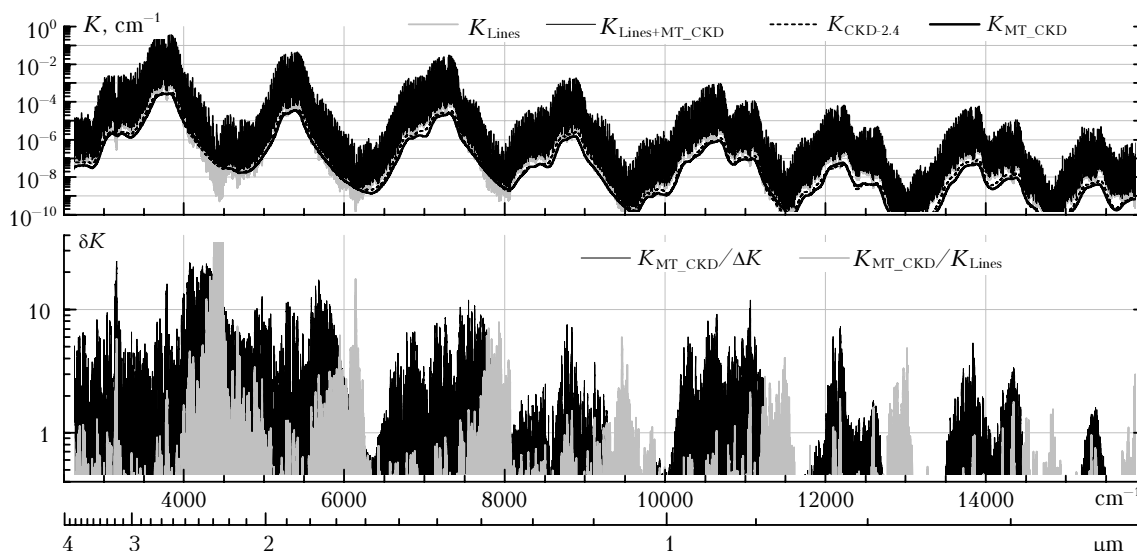


Fig. 3. Calculated water vapor absorption spectrum with and without the regard for the MT_CKD model of water continuum, along with two models of water continuum shown separately (upper panel). Ratio of the continuum absorption to the absorption by water vapor spectral lines (neglecting the continuum) and to the estimated error (ΔK) of continuum reconstruction at this frequency (bottom panel). The calculation was performed for the mixture of 20 mbar H_2O and 993 mbar of synthetic air.

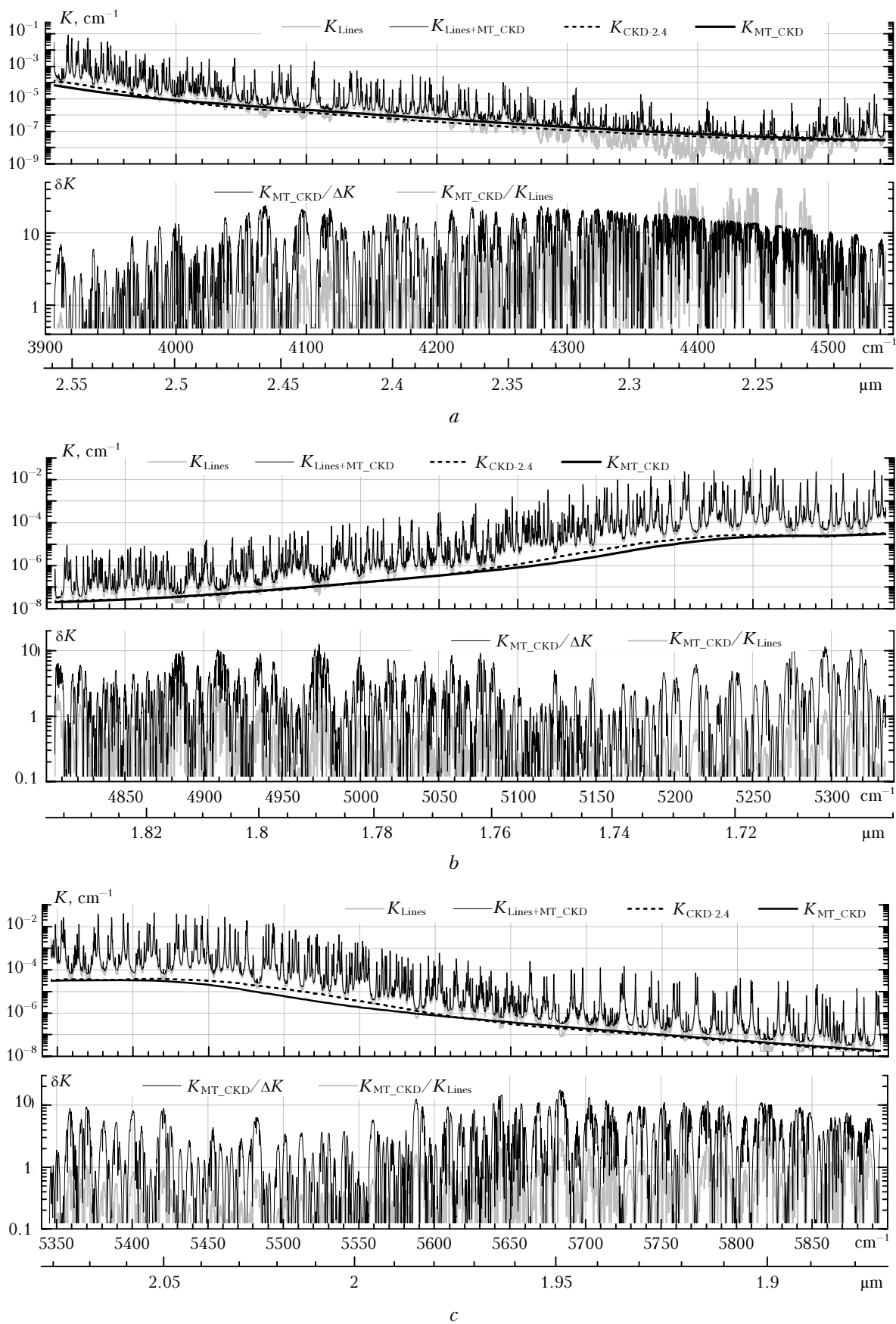


Fig. 4. The same as in Fig. 3 for the spectral regions of 3900–4550 (*a*), 4800–5350 (*b*), and 5350–5900 cm^{-1} (*c*).

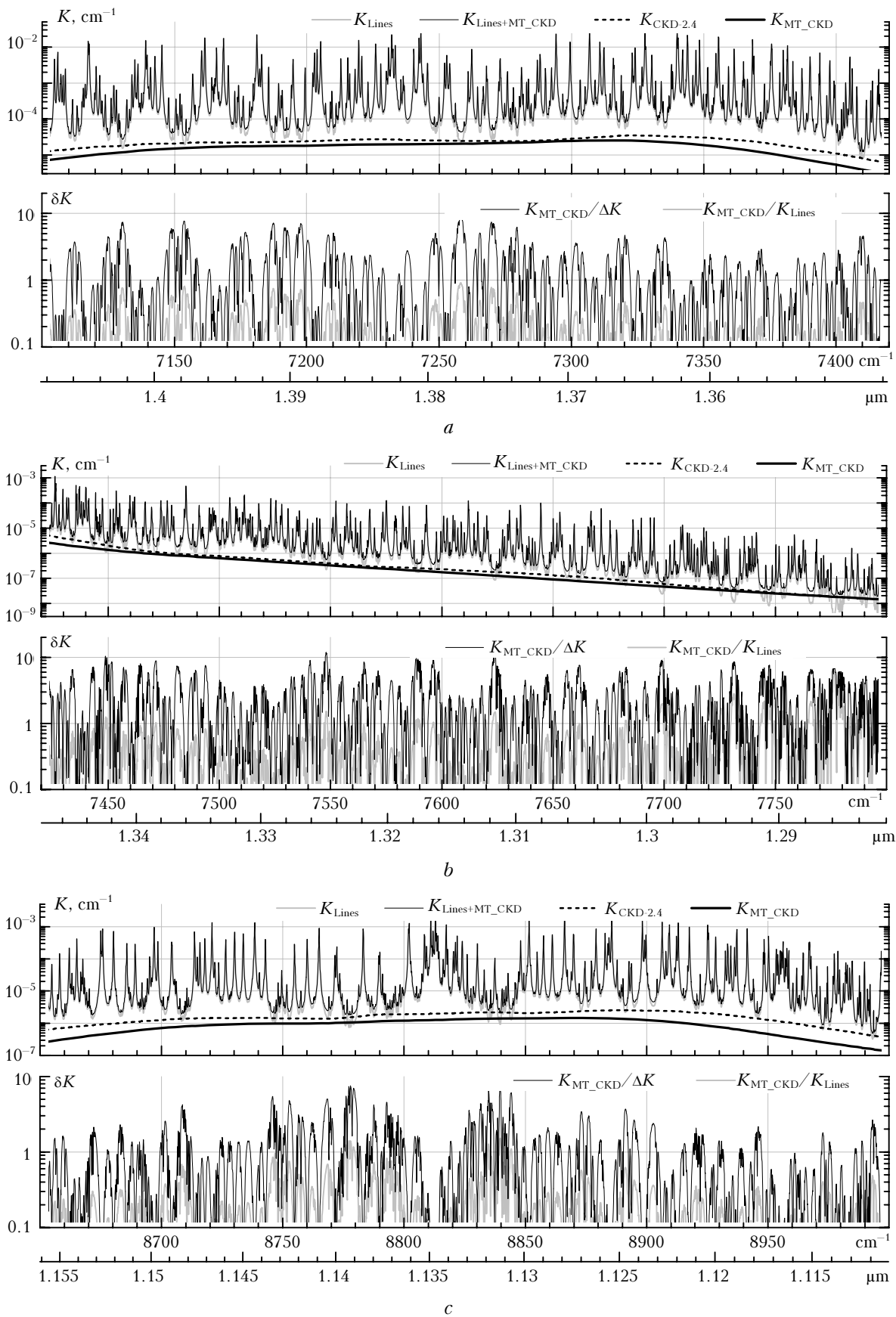


Fig. 5. The same as in Fig. 3 for the spectral regions of 7100–7420 (*a*), 7420–7800 (*b*), and 8650–9000 cm^{-1} (*c*).

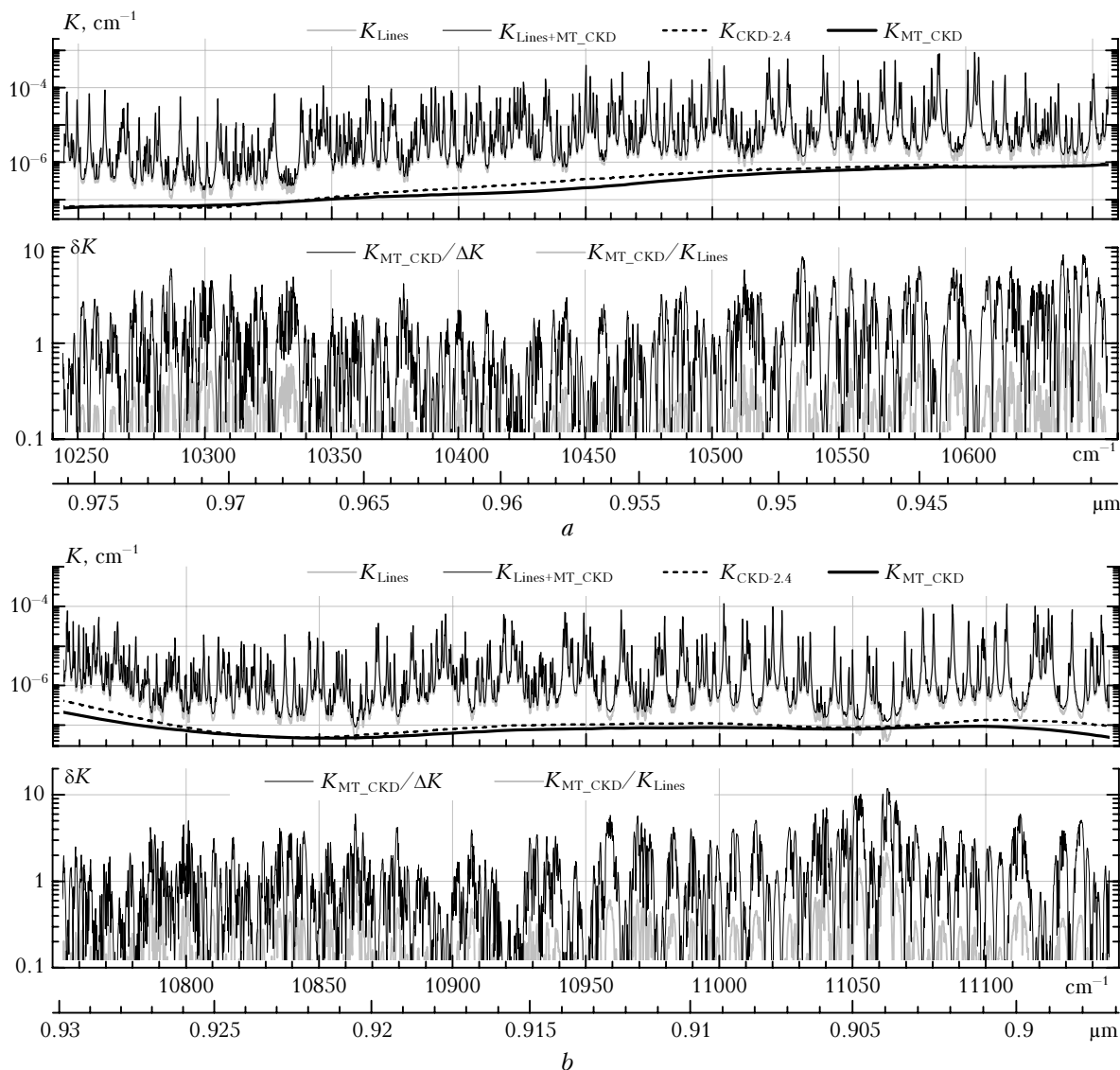


Fig. 6. The same as in Fig. 3 for the spectral regions of 10200–11200 cm^{-1} .

It should be noted that the ratio $K_{\text{MT_CKD}}/K_{\text{Lines}}$ in Figs. 3–7 characterizes the level of detectability of the continuum absorption as compared to the selective absorption by spectral lines with the continuum neglected, whereas the ratio $K_{\text{MT_CKD}}/\Delta K$ can be considered as an equivalent of the signal-to-noise ratio. Thus, spectral ranges with $K_{\text{MT_CKD}}/\Delta K > 3$ –5 can be considered as promising for the verification of the continuum with the relative error lower than 20–30%.

It has been found that the uncertainty in line parameters is the main contributor to the total error $\Delta K(\bar{\nu})$ [Eq. (2)] in the most promising ranges.

The most important uncertainties are those in line intensities, broadening coefficients, and line positions. This means that the ratios $K_{\text{MT_CKD}}/\Delta K$, shown in Figs. 3–7 can be improved (i.e., increased), if line parameters will be previously fitted (based on the experimental spectrum) in order to improve them as compared to the HITRAN-2004 and Schwenke–Partridge databases.

Conclusions

It can be seen from Figs. 3–7 that there is a large number of microwindows in the spectral ranges of 13700–13900, 12020–12260, 10200–11200, 8650–9000, 7100–7800, 4800–5900, and 3900–4550 cm^{-1} , in which we can expect a significant contribution of the continuum absorption ($K_{\text{MT_CKD}}/K_{\text{Lines}} \geq 0.5$), exceeding several times ($K_{\text{MT_CKD}}/\Delta K > 3$) possible error of its determination with a photoacoustic or cavity ring-down spectrometer. These ranges mostly correspond to centers and near wings of water vapor absorption bands. Many of these spectral ranges cover the emission ranges of diode lasers and other sources of laser radiation and, consequently, can be used for the verification of the water vapor continuum in the near IR and, partly, in the visible spectral regions.

Most of these spectral ranges can be also used for the verification of the water vapor continuum using a Fourier-transform spectrometer with a

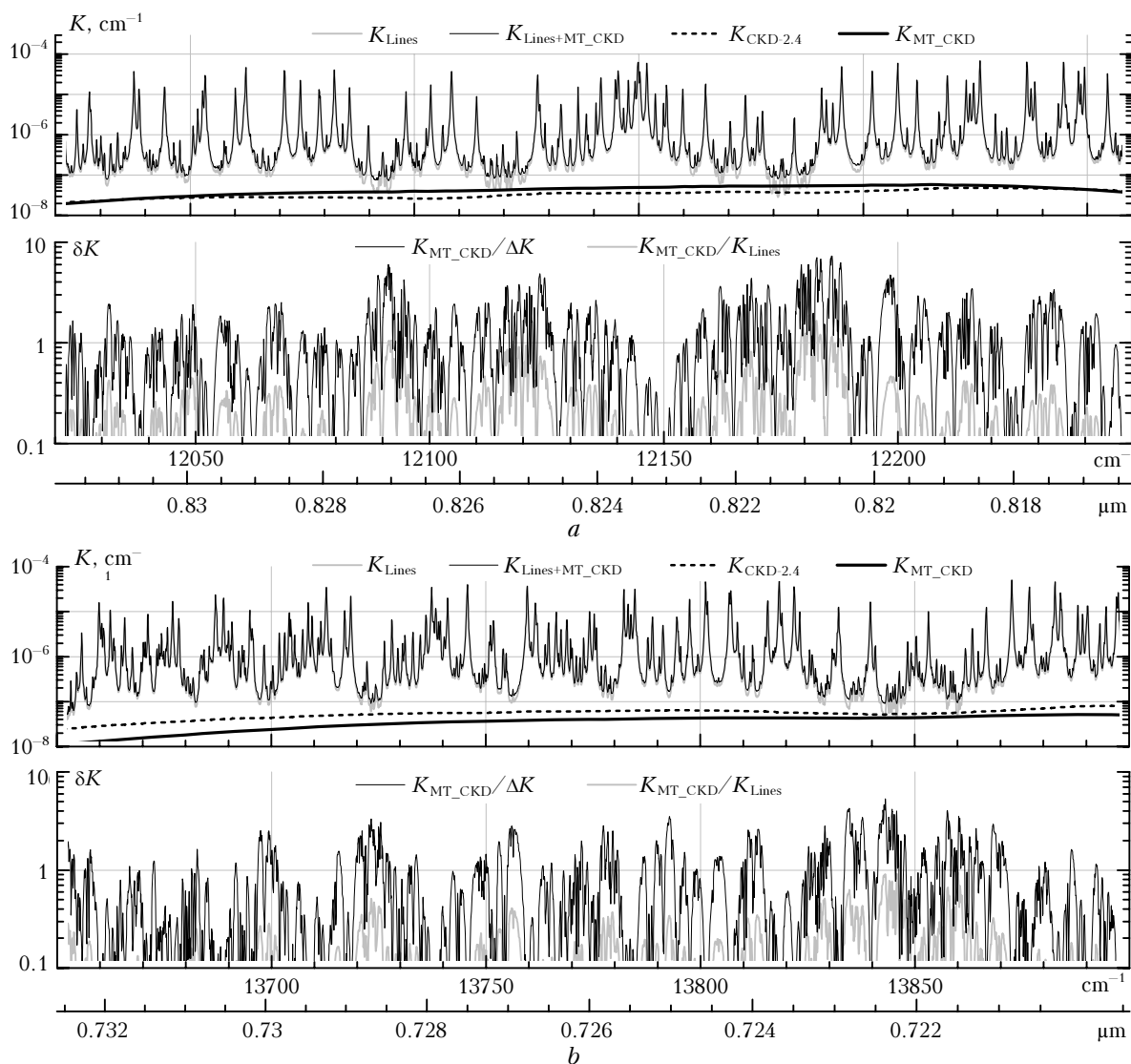


Fig. 7. The same as in Fig. 3 for the spectral regions of 12020–12250 (a) and 13650–13900 cm^{-1} (b).

multipass cell, providing for the geometrically 1000-m long optical path. The sensitivity of such a spectrometer can achieve 10^{-8} cm^{-1} .

Acknowledgments

The author is grateful to Dr. K.M. Firsov for useful recommendations in the discussion of materials presented in this paper.

This study was supported, in part, by the Russian Foundation for Basic Research (Grant No. 04–05–64569-a) and the Scientific School “Optical Spectroscopy of Molecules and Radiative Processes in the Atmosphere” (RI-112/001/020).

References

1. S.A. Clough, F.X. Kneizys, and R.W. Davies, *Atmos. Res.* **23**, 229–241 (1989).
2. E.J. Mlawer, S.A. Clough, P.D. Brown, and D.C. Tobin, in: *Ninth ARM Science Team Meeting Proc.* (San Antonio, TX, 1999), pp. 1–6.
3. E.J. Mlawer, D.C. Tobin, and S.A. Clough, *J. Quant. Spectrosc. Radiat. Transfer* (2005) (in preparation).
4. W. Zhong, J.D. Haigh, D. Belmiloud, R. Schermail, and J. Tennyson, *Quart. J. Roy. Meteorol. Soc.* **128**, No. 582, 1387–1388 (2002).
5. I.V. Ptashnik and K.P. Shine, *Atmos. Oceanic Opt.* **16**, No. 3, 251–255 (2003).
6. I.V. Ptashnik, *Atmos. Oceanic Opt.* **17**, No. 11, 795–798 (2004).
7. B.A. Fomin, T.A. Udalova, and E.A. Zhitnitskii, *J. Quant. Spectrosc. Radiat. Transfer* **86**, No. 1, 73–85 (2004).
8. D.E. Birch and R.L. Alt, in: *Rep. AFGL-TR-84-0128* (U.S. Air Force Geophysics Laboratory, 1984).
9. D.C. Tobin, L.L. Strow, W.J. Lafferty, and W.B. Olson, *Appl. Opt.* **35**, No. 24, 4724–4734 (1996).
10. Y. Han, J.A. Shaw, J.H. Churnside, P.D. Brown, and S.A. Clough, *J. Geophys. Res.* **102**, No. 4, 4353–4356 (1997).
11. D.C. Tobin, F.A. Best, P.D. Brown, S.A. Clough, R.G. De-decker, R.G. Ellingson, R.K. Garcia, H.B. Howell, R.O. Knuteson, E.J. Mlawer, H.E. Revercomb, J.F. Short, P.F. van Delst, and V.P. Walden, *J. Geophys. Res.* **104**, No. 2, 2081–2092 (1999).

12. I.V. Ptashnik, K.M. Smith, K.P. Shine, and D.A. Newnham, *Quart. J. Roy. Meteorol. Soc.* **130**, No. 602, 2391–2408 (2004).
13. I.V. Ptashnik, *Atmos. Oceanic Opt.* **18**, No. 4, 324–326 (2005).
14. J.S. Daniel, S. Solomon, H.G. Kjaergaard, and D.P. Schofield, *Geophys. Res. Lett.* **31**, L06118 (2004).
15. C. Tomasi, in: *Optical Remote Sensing of Air Pollution*, ed. by P. Camagni and S. Sandroni (Elsevier, 1983), pp. 301–327.
16. Yu.A. Pkhalagov, V.N. Uzhegov, and N.N. Shchelkanov, *Atmos. Oceanic Opt.* **11**, No. 4, 272–275 (1998).
17. L.I. Nesmelova, Yu.A. Pkhalagov, O.B. Rodimova, S.D. Tvorogov, V.N. Uzhegov, and N.N. Shchelkanov, *Atmos. Oceanic Opt.* **12**, No. 3, 278–284 (1999).
18. D.E. Birch, in: *Rep. AFGL-TR-85-0036* (U.S. Air Force Geophysics Laboratory, 1985).
19. B.A. Tikhomirov, A.B. Tikhomirov, and K.M. Firsov, *Atmos. Oceanic Opt.* **14**, No. 9, 674–680 (2001).
20. S.F. Fulghum and M.M. Tilleman, *J. Opt. Soc. Am. B* **8**, 2401–2413 (1991).
21. B. Sierk, S. Solomon, J.S. Daniel, R.W. Portmann, S.I. Gutman, A.O. Langford, C.S. Eubank, E.G. Dutton, and K.H. Holub, *J. Geophys. Res.* **109**, No. 8, D08307 (2004).
22. A.A. Mitsel', I.V. Ptashnik, K.M. Firsov, and B.A. Fomin, *Atmos. Oceanic Opt.* **8**, No. 10, 847 (1995).
23. D.W. Schwenke and H. Partridge, *J. Chem. Phys.* **113**, No. 16, 6592–6597 (2000).
24. L.S. Rothman, D. Jacquemart, A. Barbe, D. Chris Benner, M. Birk, L.R. Brown, M.R. Carleer, C. Chackerian, Jr., K. Chance, V. Dana, V.M. Devi, J.-M. Flaud, R.R. Gamache, A. Goldman, J.-M. Hartmann, K.W. Jucks, A.G. Maki, J.-Y. Mandin, S.T. Massie, J. Orphal, A. Perrin, C.P. Rinsland, M.A.H. Smith, J. Tennyson, R.N. Tolchenov, R.A. Toth, J. Vander Auwera, P. Varanasi, and G. Wagner, *J. Quant. Spectrosc. Radiat. Transfer* **95**, 139–204 (2005).